

# Simulation of a system of 2D dipolar-coupled electron spins on diamond surface

Team dark spin simulation

December 22, 2017

## **Abstract**

This is a summary of our efforts to simulate a system of 2D dipolar electron spins on the diamond surface. We are using our simulation to perform fits on the double electron-electron resonance experiments to extract spin positions as well as to try to fit other experimental results using simulation.

# 1 Overview of simulation

## 1.1 The Full Hamiltonian

The full Hamiltonian for the system of NV spin-surface spin and surface spin-surface spin magnetic dipolar interaction is given by:

$$H = H_{nv} + H_s + H_{nv-s} + H_{s-s} \quad (1)$$

$$H_{nv} = \hbar\Delta S_z^2 + \hbar\gamma_e \mathbf{B} \cdot \mathbf{S} \quad (2)$$

$$H_s = \hbar\gamma_e \mathbf{B} \cdot \sum_i \mathbf{J}_i \quad (3)$$

$$H_{nv-s} = \sum_i \frac{\hbar^2 \gamma_e^2}{r_{nv-s}^3} \left[ \mathbf{S} \cdot \mathbf{J}_i - 3 \frac{(\mathbf{S} \cdot \mathbf{r}_{nv-s})(\mathbf{J}_i \cdot \mathbf{r}_{nv-s})}{r_{nv-s}^2} \right] \quad (4)$$

$$H_{s-s} = \sum_{i>j} \frac{\hbar^2 \gamma_e^2}{r_{s-s}^3} \left[ \mathbf{J}_i \cdot \mathbf{J}_j - 3 \frac{(\mathbf{J}_i \cdot \mathbf{r}_{s-s})(\mathbf{J}_j \cdot \mathbf{r}_{ij,s-s})}{r_{s-s}^2} \right] \quad (5)$$

$\Delta = 2\pi \times 2.87$  GHz is the zero-field splitting, the  $z$ -axis points along the NV center symmetry axis,  $r_{nv-s}$  is the distance between the NV center and each surface spin, and  $r_{s-s}$  is the distance between surface spins. We have written a generic code that does not necessarily make the secular approximation for the NV center and for the surface spins, and we are able to evaluate the validity of this approximation through our simulation.

## 1.2 Approximations

We can eliminate a lot of terms for in the dipole interaction between the NV center and the surface spins by using the secular approximation with respect to the zero-field splitting. One can see this by going into a rotating frame with respect to  $\hbar\Delta S_z^2 + \hbar\gamma_e B_{nv}^z S^z$ , with  $B_{nv}^z$  being the projection of the magnetic field along the NV symmetry axis. In this rotating frame all terms linear in  $S_x$  or  $S_y$ , pick up time dependence and can be shown to average to 0 when one averages over a period. Throwing out those terms in  $H_{nv-s}$  we find:

$$H_{nv-s} \approx \sum_i \frac{\hbar^2 \gamma_e^2}{r_{nv-s}^3} \left[ S_z J_i^z - 3 \frac{(S_z z_{nv-s})(\mathbf{J}_i \cdot \mathbf{r}_{nv-s})}{r_{nv-s}^2} \right] \quad (6)$$

$$H_{nv} = 0 \quad (7)$$

where  $z_{nv-s}$  are the magnitude of the NV-surface spin distance vector projections along the NV symmetry axis. Next we can also do a secular approximation with respect to the Zeeman splitting of the surface spins. To determine which terms we throw out we must transform into a rotating frame with respect to the Zeeman term. This is easiest if we choose our quantization axis of the surface spins to be along the B field. With this choice the spin operators in the rotating frame pick up some time dependence:

$$J_i^z(t) = J_i^z \quad (8)$$

$$J_i^x(t) = J_i^x \cos(\gamma_e B t) + J_i^y \sin(\gamma_e B t) \quad (9)$$

$$J_i^y(t) = J_i^y \cos(\gamma_e B t) - J_i^x \sin(\gamma_e B t) \quad (10)$$

which is simply just a rotation by angle  $\gamma_e B t$  about the  $z$ -axis. Now the secular approximation states that our approximate Hamiltonian in this frame should be given by its time average, and therefore any terms which average to 0 over a period must be throw out. Clearly any terms linear in  $J_i^x(t)$  or  $J_i^y(t)$

will average to 0 but we must be careful about products of  $J_i^x(t)$  and  $J_i^y(t)$  as some terms cross terms might not average to 0. We will only cover the secular approximation for the surface spin interactions we refer the reader the calculation of the secular approximation for  $H_{nv-s}$  done in reference [CITE Alex PRL]. Here we list the time average of the product terms (here we denote  $\overline{(\cdot)}$  as the time average over a period):

$$\overline{J_i^x(t)J_j^y(t)} = \overline{(J_i^x \cos(\gamma_e Bt) + J_i^y \sin(\gamma_e Bt))(J_j^y \cos(\gamma_e Bt) - J_j^x \sin(\gamma_e Bt))} = \frac{1}{2} (J_i^x J_j^y - J_i^y J_j^x) \quad (11)$$

$$\overline{J_i^x(t)J_j^x(t)} = \overline{(J_i^x \cos(\gamma_e Bt) + J_i^y \sin(\gamma_e Bt))(J_j^y \cos(\gamma_e Bt) - J_j^x \sin(\gamma_e Bt))} = \frac{1}{2} (J_i^x J_j^y + J_i^y J_j^x) \quad (12)$$

$$\overline{J_i^y(t)J_j^y(t)} = \overline{(J_i^y \cos(\gamma_e Bt) - J_i^x \sin(\gamma_e Bt))(J_j^y \cos(\gamma_e Bt) - J_j^x \sin(\gamma_e Bt))} = \frac{1}{2} (J_i^x J_j^y + J_i^y J_j^x). \quad (13)$$

Now collecting all the left over terms (note that  $\mathbf{J}_i \cdot \mathbf{J}_j$  is invariant under global rotations):

$$H_{s-s} = \sum_{i>j} \frac{\hbar^2 \gamma_e^2}{r_{s-s}^3} \left[ \mathbf{J}_i \cdot \mathbf{J}_j - 3 \frac{(\mathbf{J}_i \cdot \mathbf{r}_{s-s})(\mathbf{J}_j \cdot \mathbf{r}_{s-s})}{r_{s-s}^2} \right] \approx \sum_{i>j} \frac{\hbar^2 \gamma_e^2}{r_{s-s}^3} \left[ \mathbf{J}_i \cdot \mathbf{J}_j - \frac{3}{r_{s-s}^2} \left( z_{s-s}^2 J_i^z J_j^z + \frac{x_{s-s}^2 + y_{s-s}^2}{2} (J_i^x J_j^x + J_i^y J_j^y) \right) \right] \quad (14)$$

which one can recognize as a anisotropic Heisenberg interaction with effective couplings:

$$H_{s-s} = \sum_{i>j} J_{zz}(\mathbf{r}_{s-s}, \mathbf{B}) J_i^z J_j^z + J_{xy}(\mathbf{r}_{s-s}, \mathbf{B}) (J_i^x J_j^x + J_i^y J_j^y) \quad (15)$$

$$J_{zz}(\mathbf{r}_{s-s}, \mathbf{B}) = \frac{\hbar^2 \gamma_e^2}{r_{s-s}^3} (1 - 3 \cos^2(\theta_{r-B})) \quad (16)$$

$$J_{xy}(\mathbf{r}_{s-s}, \mathbf{B}) = \frac{\hbar^2 \gamma_e^2}{r_{s-s}^3} \left( 1 - \frac{3}{2} \sin^2(\theta_{r-B}) \right). \quad (17)$$

with  $\theta_{r-B}$  being the angle between  $\mathbf{r}_{s-s}$  and  $\mathbf{B}$ . Since all our surface spins are in the same plane that means this angle is just the angle the B-field makes with the surface, lets call  $\theta_{||}$ . Combining all of the terms we find our final Hamiltonian:

$$H = S_z \sum_i \hbar k_i J_i^z + \sum_{i>j} J_{ij}^{zz}(\theta_{||}) J_i^z J_j^z + J_{ij}^{xy}(\theta_{||}) (J_i^x J_j^x + J_i^y J_j^y) \quad (18)$$

where  $k_i$  are defined in reference [CITE Alex PRL]. Rearranging terms, we find that our final Hamiltonian takes the following form:

$$H = S_z \sum_i \hbar k_i J_i^z + \frac{1}{2} \sum_{i>j} J_{ij}^{zz}(\theta_{||}) (2 J_i^z J_j^z - J_i^x J_j^x - J_i^y J_j^y) \quad (19)$$

### 1.3 DEER Pulse Sequence Solution

Next we will discuss the exact solution for two surface spins but first let us calculate the Results of the Pulse sequence for  $N_s$  spins which we will then use to calculate an exact expression for the 2-surface spin case. In the experiment the NV center is initially populated in the  $m_S = 0$  state while our surface spins begin in an infinite temperature state. For the following analysis though we will consider the surface spins to be in an arbitrary pure state to make the calculation simpler but we will show how the expression generalizes to an arbitrary initial density matrix after the calculation is complete. In this section we will set  $\hbar = 1$ . To begin we start with our state of the system in a product state of the NV center and the surface spin state:

$$|\psi_0\rangle = |0\rangle |\psi_s\rangle. \quad (20)$$

The DEER pulse sequence begins with a  $\pi/2$  rotation about the  $y$ -axis acting only on the NV center which leads to:

$$|\psi_1\rangle \equiv U_{\pi/2}|\psi(0)\rangle = U_{\pi/2}|0\rangle|\psi_s\rangle = \frac{1}{\sqrt{2}}(|0\rangle|\psi_s\rangle + |-1\rangle|\psi_s\rangle), \quad (21)$$

which is then followed by a period where the system evolves under its own dynamics. We will approximate these dynamics using the Hamiltonian under secular approximation derived in the previous section. Since this Hamiltonian is diagonal with respect to the NV center, therefore the two terms in the expression above are effectively two copies of the surface spins evolving under two Hamiltonians which depend only in the project of the NV center. So we will define the evolution operator on the surface spin Hilbert space with different  $S_z$  projections:

$$U_t^{S_z} = \exp \left[ -i(t/2) \left( S^z \sum_i k_i J_i^z + H_{s-s} \right) \right] \quad (22)$$

where  $S = -1, 0$  or  $1$  for the different projections allowed and  $H_{s-s}$  is the surface spin interaction term. With this now we can evolve our state:

$$|\psi_2\rangle \equiv e^{-itH}|\psi_1\rangle = e^{-itH} \frac{1}{\sqrt{2}}(|0\rangle|\psi_s\rangle + |-1\rangle|\psi_s\rangle) = \frac{1}{\sqrt{2}}(|0\rangle(U_t^0|\psi_s\rangle) + |-1\rangle(U_t^{-1}|\psi_s\rangle)). \quad (23)$$

Next we apply a  $\pi$  rotation about the  $y$ -axis on both the surface spins and the NV center:

$$|\psi_3\rangle \equiv U_\pi|\psi_2\rangle = \frac{1}{\sqrt{2}}(|-1\rangle(U_\pi U_t^0|\psi_s\rangle) - |0\rangle(U_\pi U_t^{-1}|\psi_s\rangle)) \quad (24)$$

followed by another round of dynamics:

$$|\psi_5\rangle \equiv e^{-itH}|\psi_4\rangle = \frac{1}{\sqrt{2}}(|-1\rangle(U_t^{-1}U_\pi U_t^0|\psi_s\rangle) - |0\rangle(U_t^0U_\pi U_t^{-1}|\psi_s\rangle)). \quad (25)$$

Followed by another  $\pi/2$  rotation acting on the NV center. Defining  $|\psi_s(t)\rangle = U_t^0 U_\pi U_t^{-1}|\psi_s\rangle$  and  $|\tilde{\psi}_s(t)\rangle = U_t^{-1} U_\pi U_t^0|\psi_s\rangle$  our final state is now:

$$|\psi_f\rangle = \frac{1}{2} \left[ -|0\rangle (|\tilde{\psi}_s(t)\rangle + |\psi_s(t)\rangle) + |-1\rangle (|\psi_s(t)\rangle - |\tilde{\psi}_s(t)\rangle) \right] \quad (26)$$

If we measure the occupation in the  $|0\rangle$  state we find it is given by:

$$S = \frac{1}{2} \left[ 1 + \text{Re} \left( \langle \psi_s | U_t^{-1\dagger} U_\pi^\dagger U_t^{0\dagger} U_t^{-1} U_\pi U_t^0 | \psi_s \rangle \right) \right] \quad (27)$$

Where we note that our interaction Hamiltonian is invariant under rotations by  $\pi$  about the  $y$ -axis so we can simplify this to:

$$S = \frac{1}{2} \left[ 1 + \text{Re} \left( \langle \psi_s | U_t^{-1\dagger} U_t^{0\dagger} U_t^1 U_t^0 | \psi_s \rangle \right) \right]. \quad (28)$$

Now we can express this in terms of a density matrix by inserting a complete set of states and rearranging terms to get:

$$S = \frac{1}{2} \left[ 1 + \text{Re} \left( \text{Tr}(U_t^1 U_t^0 \rho_s U_t^{-1\dagger} U_t^{0\dagger}) \right) \right] \quad (29)$$

which if we start out in an infinite temperature state reduces to:

$$S = \frac{1}{2} \left[ 1 + \frac{1}{2^{N_s}} \text{Re} \left( \text{Tr}(U_t^1 U_t^0 U_t^{-1\dagger} U_t^{0\dagger}) \right) \right] \quad (30)$$

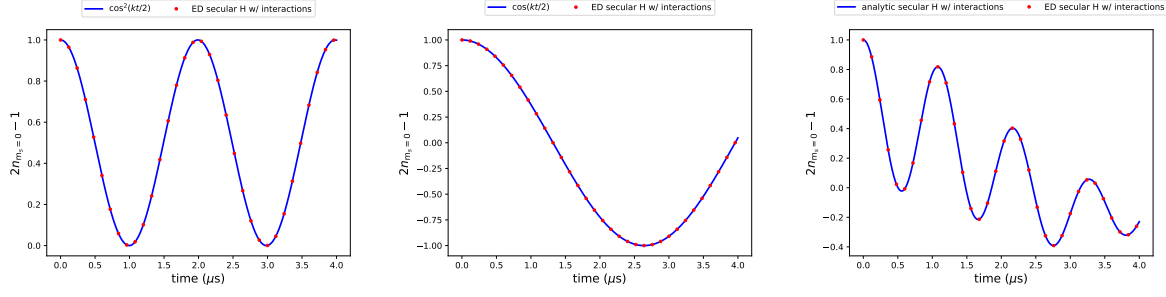


Figure 1: Comparison with exact numerical code and analytic solution in two limits. (left) surface spins on surface at position  $r_1 = (1, -0.1, 2.8)$  and  $r_1 = (1, 0.1, 2.8)$ . In this limit we expect that  $k_1 = k_2$  which the interactions don't matter. (center) surface spins on surface at position  $r_1 = (-2, -1, 2.8)$  and  $r_1 = (0.6, 0.1, 2.8)$ . In this limit interactions plays a role. (right) surface spins on surface at position  $r_1 = (0, 0, 2.8)$  and  $r_1 = (100, 100, 2.8)$ . In this limit there is effectively only one spin and the curve should reduce to the non-interacting case. All distances are in nanometers.

where  $N_s$  is the total number of surface spins. Note that in the non-interacting limit  $H_{s-s} \rightarrow 0$  and we recover the exact expression as in Ref [Cite Alex PRL] (up to a factor of 2 which is due to the fact that we evolve the system for a period of  $t$  not  $t/2$  between pulses.):

$$S = \frac{1}{2} \left[ 1 + \frac{1}{2^{N_s}} \text{Re} \left( \text{Tr} (e^{-it \sum_j k_j J_j^z}) \right) \right] = \frac{1}{2} \left[ 1 + \prod_j \cos(tk_j/2) \right] \quad (31)$$

Now that we have our general expression we can move on to the two surface spin solution. The Full Hamiltonian for this system is given by:

$$H = S_z(k_1 J_1^z + k_2 J_2^z) + \frac{1}{2} J_{12}^{zz}(\theta_{||}) \left[ 2J_1^z J_2^z - \frac{1}{2} (J_1^+ J_2^- + J_1^- J_2^+) \right] \quad (32)$$

where we have written the  $x$  and  $y$  terms in raising and lowering operators. From this form you can see that the  $|\uparrow\uparrow\rangle$  and  $|\downarrow\downarrow\rangle$  states are eigenstates of  $H$  while in the subspace of  $J_1^z + J_2^z = 0$  we have an effective hamiltonian given by:

$$H_{J_1^z + J_2^z = 0} = -\frac{J_{12}^{zz}(\theta_{||})}{4} (1 + \sigma_x) + \frac{S^z}{2} (k_1 - k_2) \sigma_z \quad (33)$$

One can easily work out the evolution operators for each value of  $S^z$  and perform the trace in Eq. (30) which leads to:

$$S_2(t) = \frac{1}{8} \left\{ \frac{4(k_1 - k_2)^2}{J_{12}^{zz}(\theta_{||})^2 + 4(k_1 - k_2)^2} \left[ \cos \left( \frac{t}{4} \sqrt{J_{12}^{zz}(\theta_{||})^2 + 4(k_1 - k_2)^2} \right) - 2 \cos \left( \frac{J_{12}^{zz}(\theta_{||})t}{4} \right) \sin^2 \left( \frac{t}{8} \sqrt{J_{12}^{zz}(\theta_{||})^2 + 4(k_1 - k_2)^2} \right) \right] + \frac{J_{12}^{zz}(\theta_{||})^2}{J_{12}^{zz}(\theta_{||})^2 + 4(k_1 - k_2)^2} + 2 \cos \left( \frac{1}{2} (k_1 + k_2) t \right) + 5 \right\} \quad (34)$$

## 1.4 General Calculation procedure

We begin our simulation by defining an initial density matrix containing the initial NV center spin state in the  $m_s = 0$  magnetic spin sublevel and define the initial state of our surface spins as existing in an infinite temperature bath. We then define our pulse sequence as consisting of rotation operators that

act on either two of the NV spin states or the surface spin bath as well as unitary evolution operators which evolve the system under the given Hamiltonian for a specified amount of time. We determine the final density matrix of our system by performing the operation  $U_{seq}\rho_{init}U_{seq}^t$ . We then determine what our measurement outcome will be by taking the trace of our measurement operator (defined to be the population in the NV  $m_s = 0$  spin state) with the final density matrix.

## 2 Simulation results for the case of two surface spins

With an analytic solution in hand, we can begin to gain a better intuition for what signal two surface spins will produce.

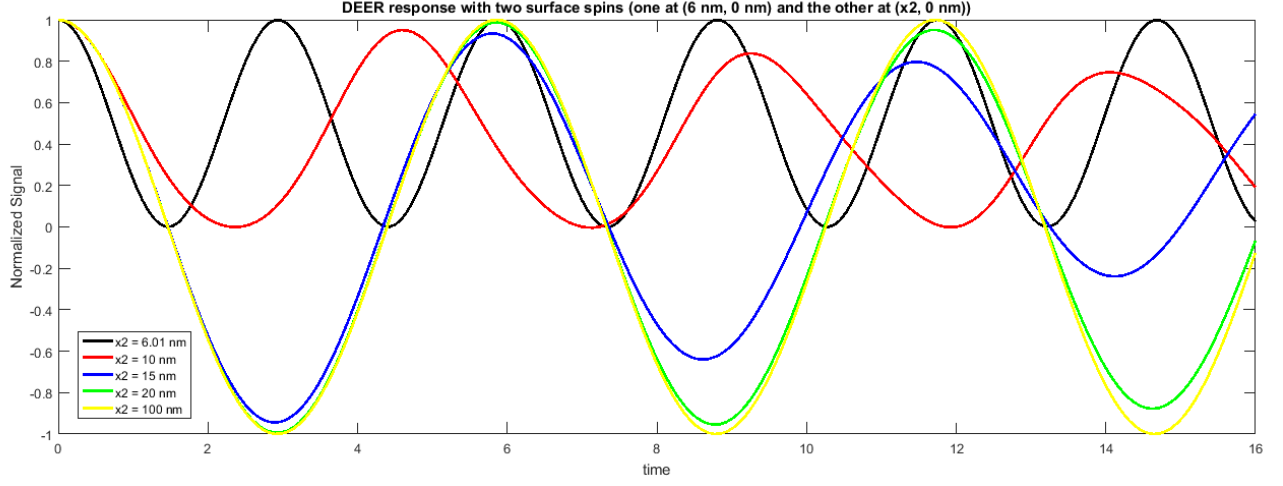


Figure 2: Simulation results for two surface spins, varying the x-coordinate of one. The NV center depth is 2.8 nm. The position of the first spin is fixed at (6 nm, 0 nm) and the y-coordinate of the second spin is fixed at 0 nm. When the surface spins are located close together, the DEER result goes as  $\cos(kt)^2$  and when one spin is placed far away from the NV, the result goes as  $\cos(kt)$ .

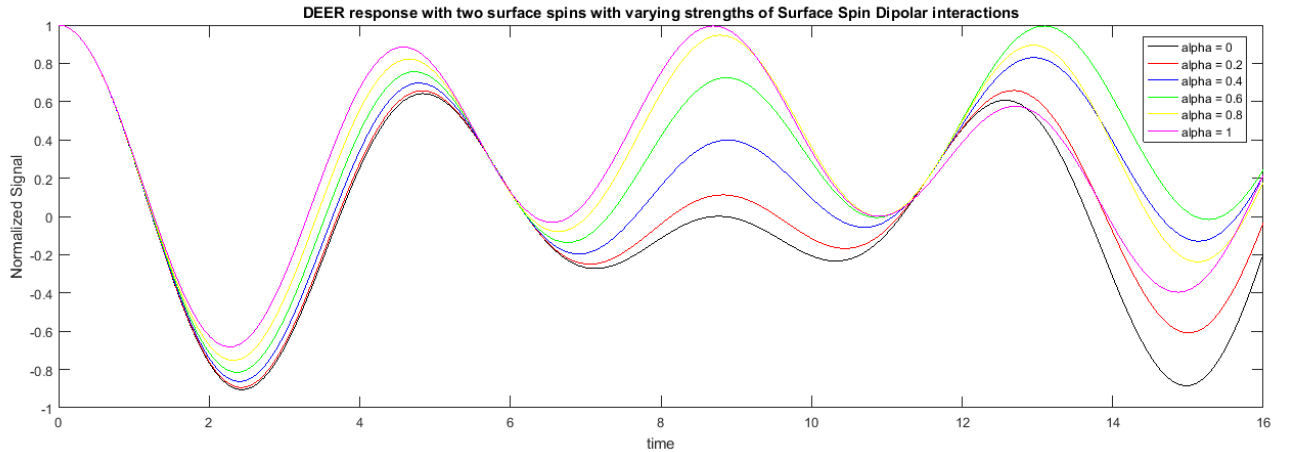


Figure 3: Simulation results for two surface spins, varying a parameter alpha which the dipolar interaction between surface spins is multiplied by. Tuning alpha to 1 turns on the full dipolar interaction, and tuning alpha to 0 turns off the dipolar interaction. The NV depth is 2.8 nm and the surface spin positions are (0,3) and (0,9) nm. We find that including the dipolar interaction between surface spins greatly changes the DEER result at later times.

### 3 Evaluating Error in Magnet Angles

For small magnetic field offsets from the NV axis, there is an error of 5 degrees in the precision with which we can measure our magnetic field offset. Plotted below is the result of the DEER measurement for surface spin positions  $(-0.42, -0.31)$ ,  $(4.5, 1.7)$ ,  $(2.1, -4.6)$ , and  $(6.8, -2.8)$  and with an NV depth of 2.78, all distances given in nanometers. We vary the angle  $\phi$  for different values to show that for small angles, a miscalibration in  $\phi$  produces DEER results that are within the error bars of about 0.1 on the scale shown in all of the figures.

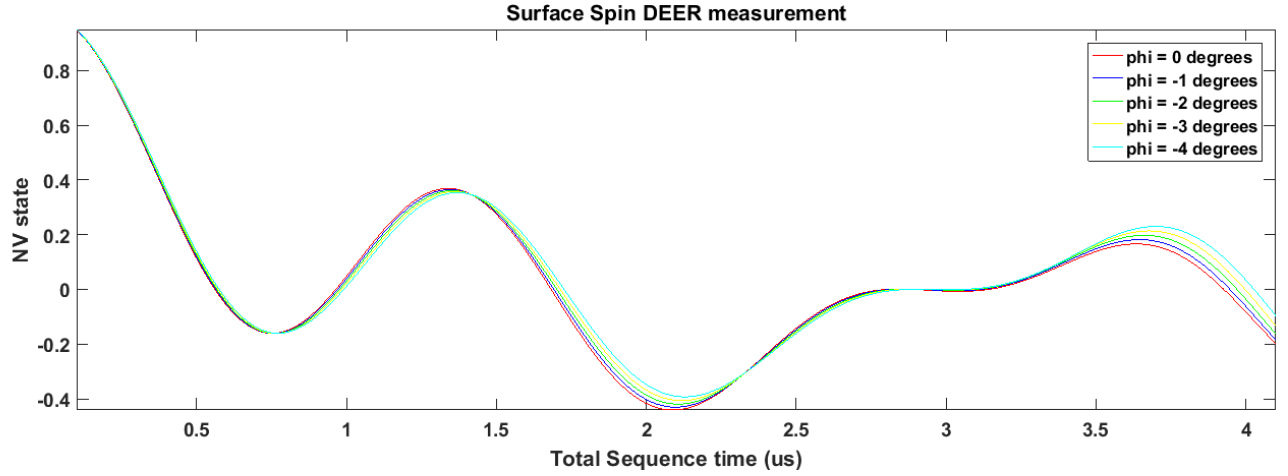


Figure 4: DEER results for 4 spins at different magnetic field offsets from the NV axis. Note to Kristine: I need to fix the title as it should just say "DEER measurement" since this measurement was done on the NV and not the surface spins.

For our measurements with large magnetic field offset from the NV axis, the accuracy with which we can measure our angle offsets has an error of about 2 degrees. Plotted below are the results of DEER measurements for larger magnetic field offsets. For these larger angles, a difference of 2 degrees makes a difference larger than the error bar of our measurements.

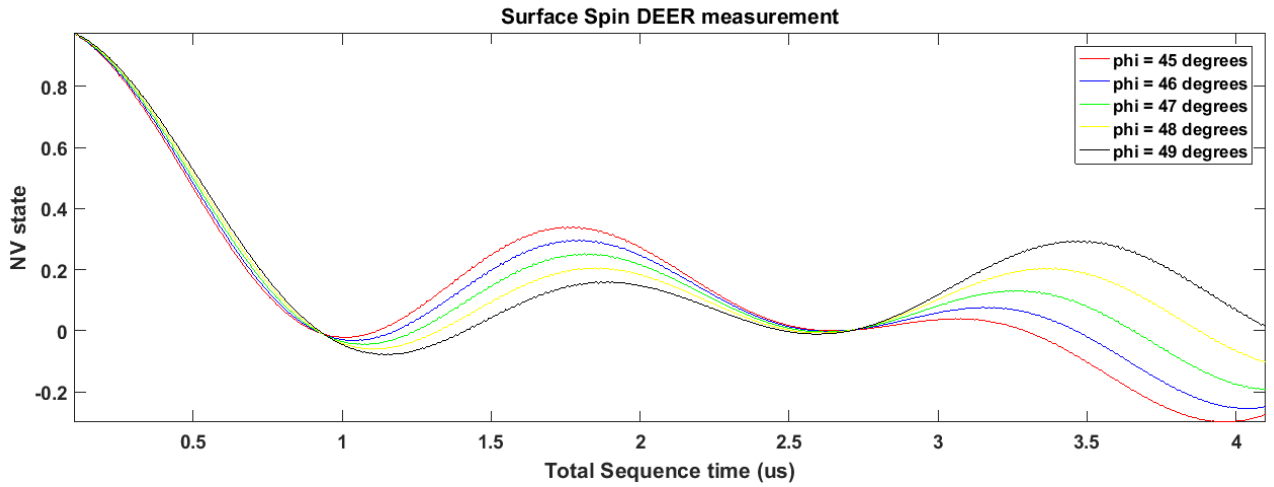


Figure 5: DEER results for 4 spins at different magnetic field offsets from the NV axis. Note to Kristine: I need to fix the title as it should just say "DEER measurement" since this measurement was done on the NV and not the surface spins.

In our measurements, we only change the relative angle of phi and assume that we have a theta that is 0 degrees (our angles are 54.7 degrees from the vertical, along the NV axis). Below is a plot of different theta offsets, assuming the same surface spin positions and NV depth as before. We set phi to be 45 degrees.

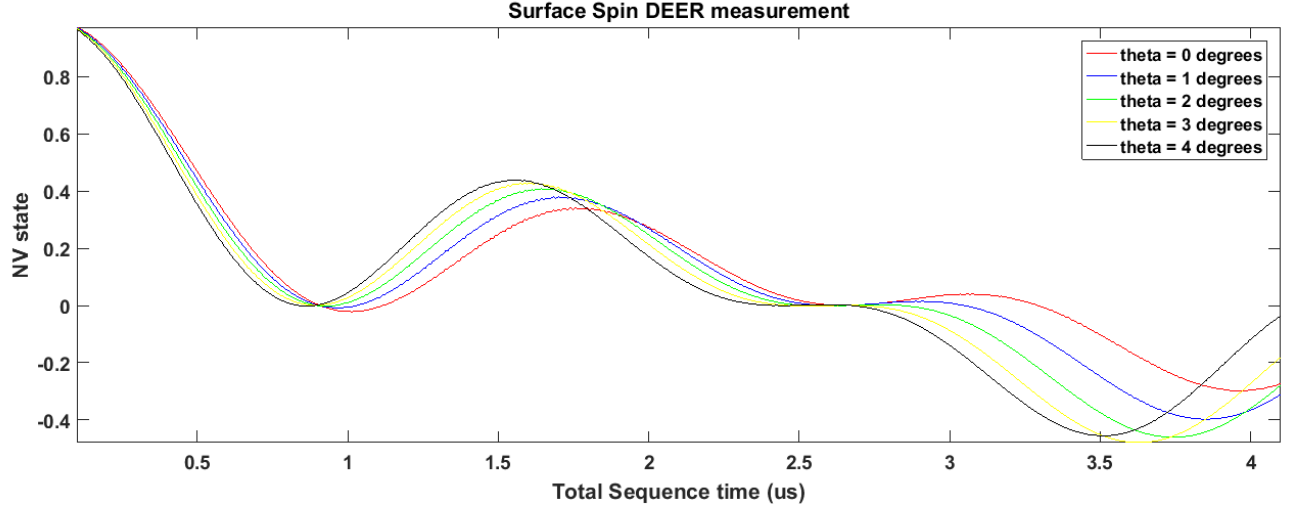


Figure 6: DEER results for 4 spins at different magnetic field offsets from the NV axis. Note to Kristine: I need to fix the title as it should just say "DEER measurement" since this measurement was done on the NV and not the surface spins.

## 4 Using simulation to extract surface spin locations

### 4.1 Fit to 3 surface spins

We fit all of our DEER measurements together to 3 surface spins, starting with fitting to the analytic solution considering only the NV-surface spin dipolar interaction and fine-tuning each position to the fit with the full Hamiltonian. Figure 7 displays the result of these fits to our measurements. The depth of this NV center is 2.74 nm and the positions of each of our surface spins in nanometers are  $(-.33, 2)$ ,  $(-1.7, -5.5)$ , and  $(4.7, -1)$ . The chi-squared per point is .011.



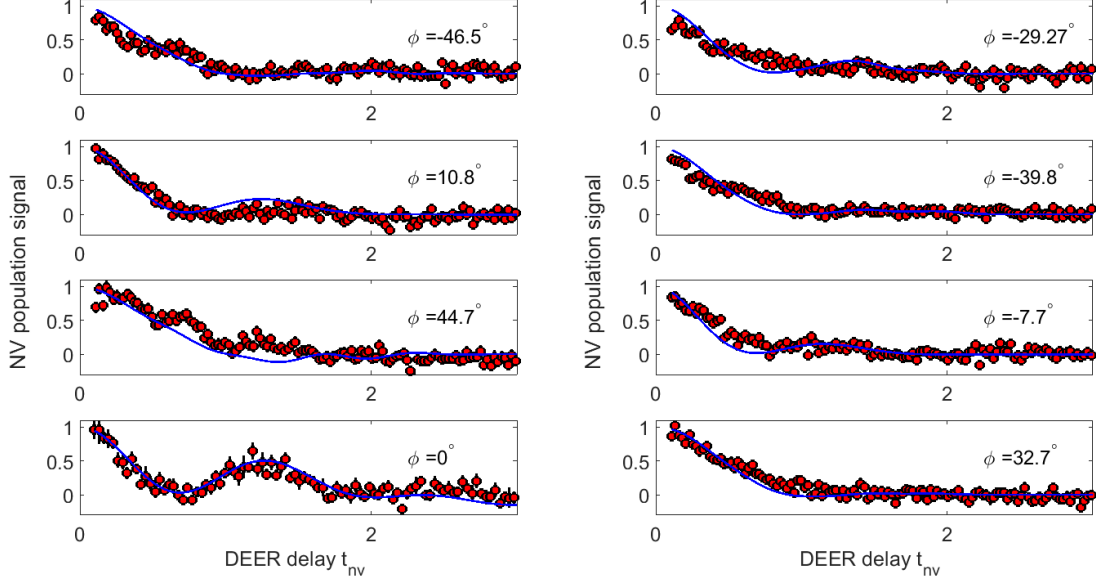
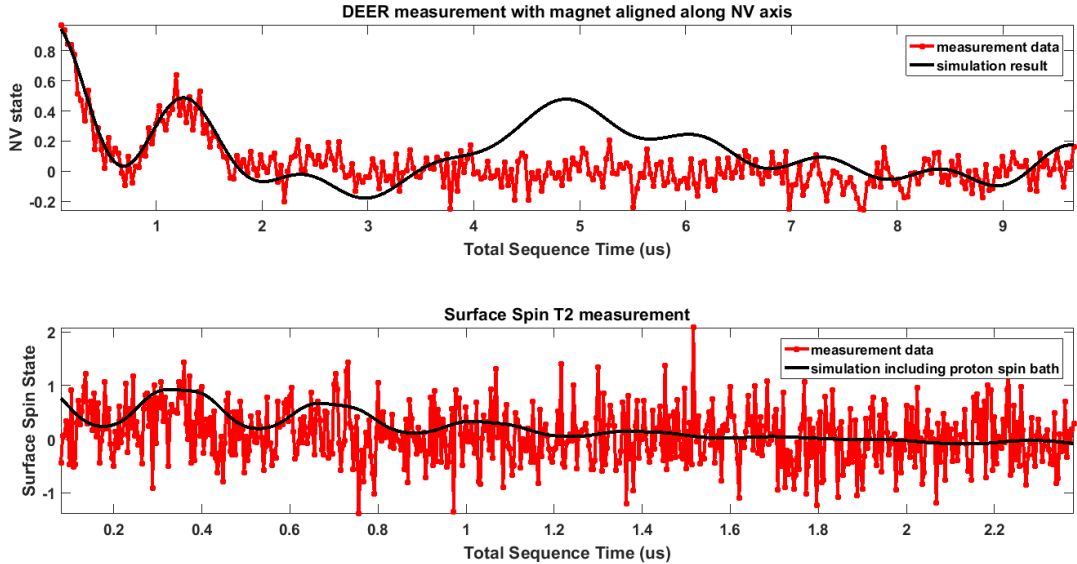
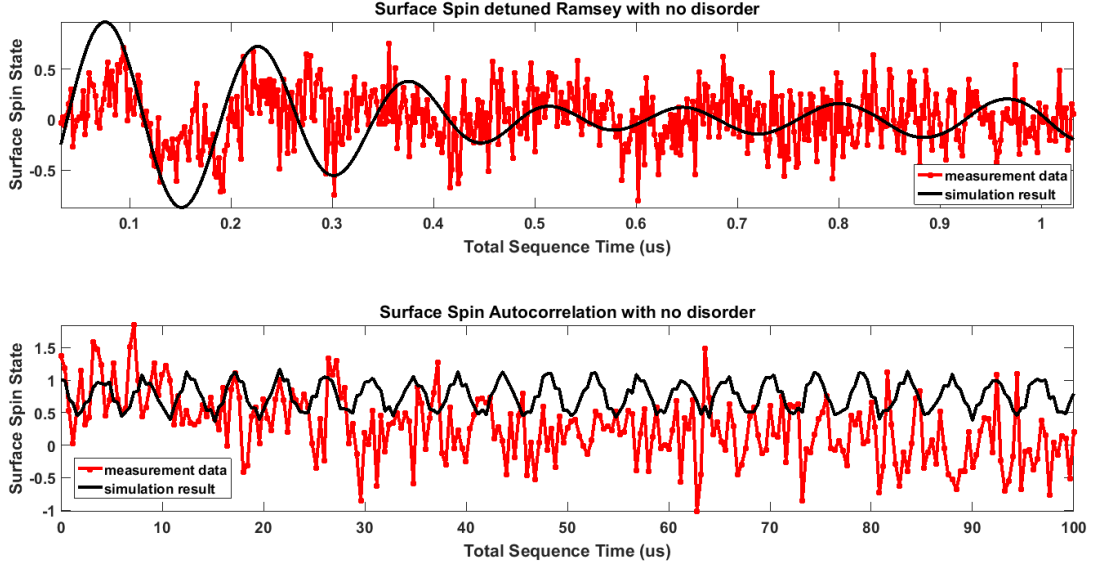


Figure 7: DEER data taken at 8 different magnet angles. The magnetic field amplitude was  $\approx 45$  Gauss.

Using these positions, we can simulate the result of our different pulse sequences using the fully interacting Hamiltonian in the secular approximation. We choose a short time between NV pulses in our correlation spectroscopy sequence such that we are strongly coupled to one surface spin and more weakly coupled to the rest. In addition, we choose a time between initial NV pulses and readout NV pulses that is much longer than our NV  $T_2^*$  time such that our surface spin state is stored in the NV z-projection.





From our detuned Ramsey, we can infer that we need time-dependent disorder in order to get a faster decay. We can repeat the same fully-interacting simulation with the presence of time-dependent disorder of varying strengths in order to extract the appropriate disorder width.

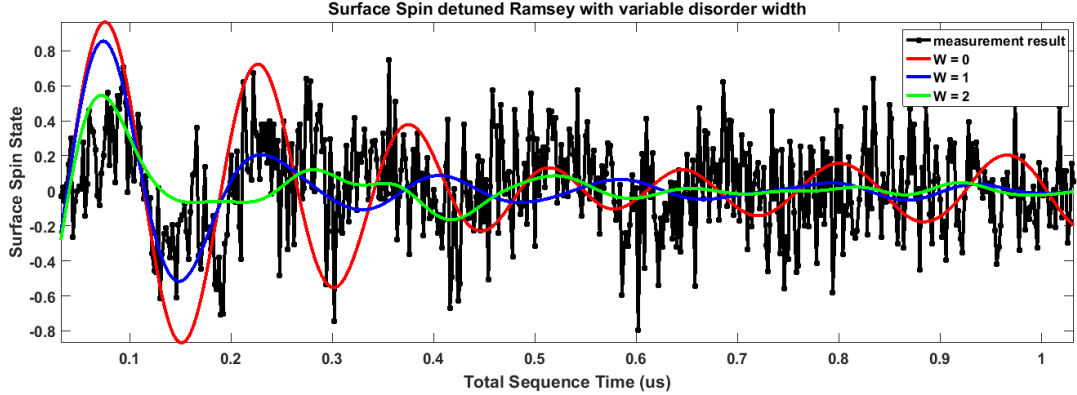


Figure 8: Detuned Ramsey simulation results for various disorder widths. The disorder width is given in MHz. Each simulation curve is the result of the average of 20 runs with different values of disorder taken from a standard normal distribution multiplied by the disorder width.

From these fits, a disorder width of about 1 MHz approximately fits the decay in the data, which does contradict my approximated disorder width of 2.8 MHz from fitting an exponential decay to my  $T_2$  and  $T_2^*$ .

We can go ahead and run these simulations with a disorder width of 1 MHz and see how well the simulation reproduces experimental results.

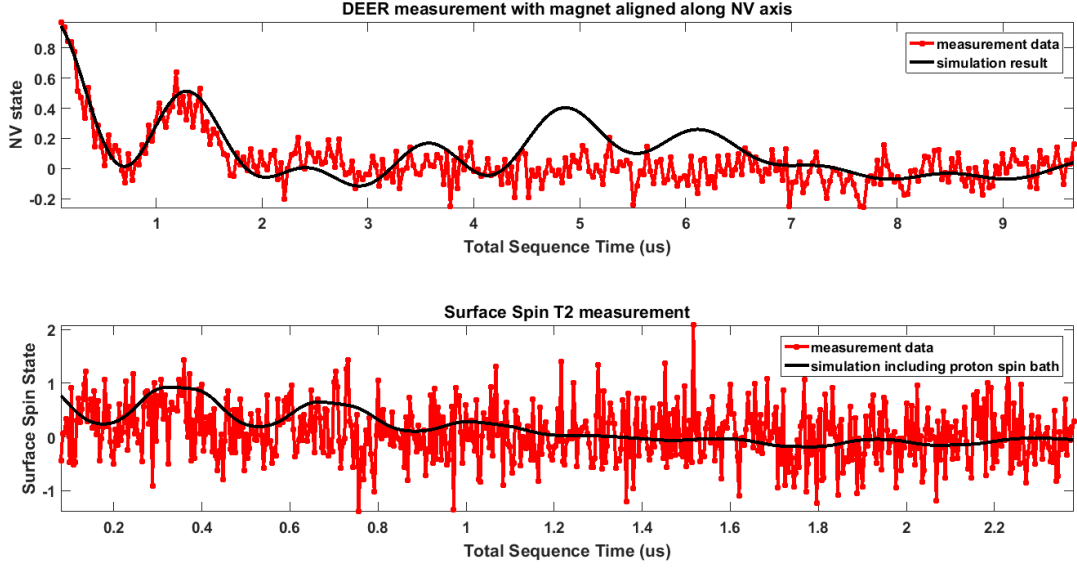


Figure 9: Result of double electron-electron resonance sequence (top) and a surface spin echo sequence (bottom) in the presence of a 1 MHz disorder width.

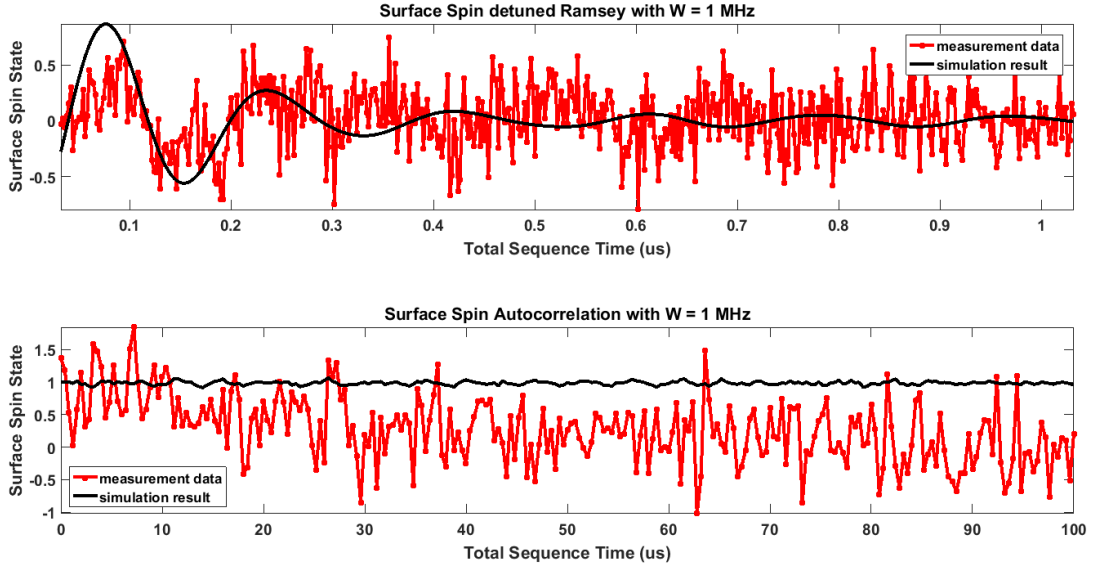


Figure 10: Result of a detuned Ramsey sequence on the surface spin as well as a surface spin autocorrelation measurement in the presence of a 1 MHz disorder width.

With the addition of time-varying disorder, our model predicts that the strongest coupled electronic spin has localized, which may be the case if there are only 3 spins on the surface present, but our experimental results show that this is not the case. We need to include the presence of all of the electronic spins on the surface, but since we cannot localize more than 3 or 4, we will calculate the relaxation rate given a spin bath located outside away from our localized spins.

The relaxation due to a single other surface spin is given by

$$\gamma(r) = \frac{J_0}{r^3} \quad (35)$$

where  $J_0$  is the interaction strength (52 MHz  $nm^3$  for electronic spins) and  $r$  is the distance separating the surface spins. In the presence of disorder, the probability of two spins being on resonance is given by  $\alpha \frac{J_0/r^3}{W}$  where  $W$  is the disorder width and  $J_0$  and  $r$  are previously defined.  $\alpha$  is a free parameter encompassing the resonance condition and is valued around 1. Incorporating this resonance condition, the relaxation due to a single other surface spin is given by

$$\gamma(r) = \alpha \frac{J_0^2}{W r^6} \quad (36)$$

The above expression provides the expected relaxation rate due to a single other surface spin, but we will calculate the relaxation due to all other surface spins with density  $n_s$  a specified distance  $a$  away from the strongest coupled surface spin.

$$\gamma(r) = \int_a^\infty \frac{\alpha J_0}{W r^6} n_s 2\pi r dr = \frac{\pi \alpha J_0 n_s}{2W a^4} \quad (37)$$

We can also relate the density of surface spins  $n_s$  to the starting distance of the bath  $a$  by

$$n_s = \frac{3}{2\pi a^2} \quad (38)$$

Using this expression, we can vary the values of  $a$  and  $\alpha$  to see if we get a good fit to our experimental results, the results of which are shown in the figure below.

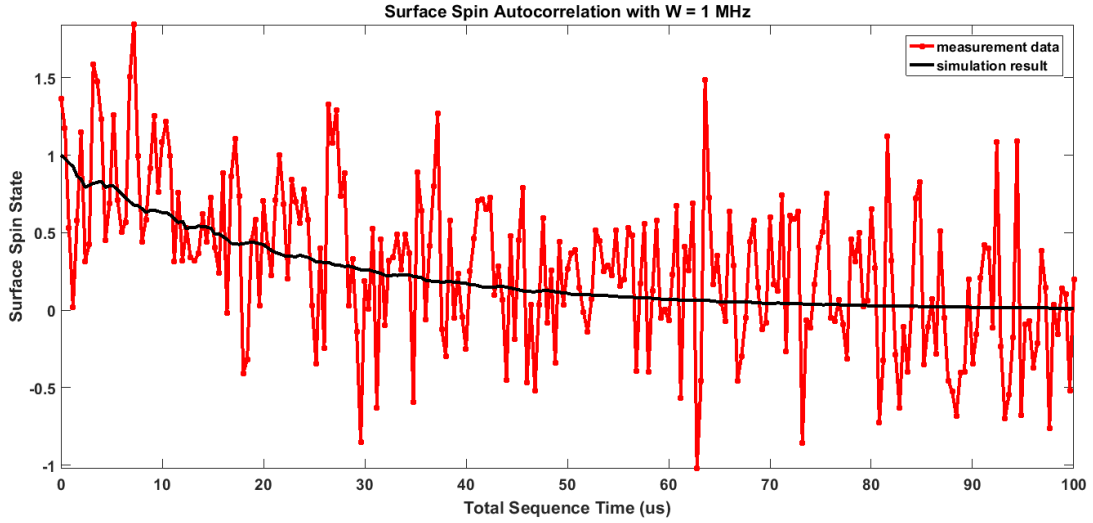


Figure 11: Surface spin autocorrelation measurement with simulation results multiplied by an exponential decay given by  $\gamma$  in the equation above. We set the bath to be 6 nm away from the most strongly coupled surface spin.  $\alpha$  is set to 1.